

Applicability of constitutive relations from kinetic theory for dense granular flows

K. Anki Reddy and V. Kumaran

Department of Chemical Engineering, Indian Institute of Science, Bangalore 560 012, India

(Received 2 March 2007; published 27 December 2007)

The applicability of constitutive models based on kinetic theory for dense granular flows is examined. First, we calculate the average coordination number of a particle in a dense flow down an inclined plane using discrete element simulations that employ a linear spring-dashpot model for particle interactions. It is found that the average coordination number decreases as the spring constant increases at constant coefficient of restitution, and is less than 1 for the values of spring constant corresponding to materials such as sand and glass beads. The Bagnold coefficients, which are the ratios of the different components of the stress and the square of the strain rate, are calculated using both discrete element (DE) simulations and event driven (ED) simulations; collisions are considered to be instantaneous in the latter simulations. It is found that the theoretical predictions of the Bagnold coefficients are in quantitative agreement with both DE and ED simulations provided the pair distribution function obtained from the simulations is inserted into the theory. However, it is found that the pair distribution function in a sheared granular flow is significantly larger than that in an equilibrium fluid of elastic particles.

DOI: [10.1103/PhysRevE.76.061305](https://doi.org/10.1103/PhysRevE.76.061305)

PACS number(s): 45.70.Mg, 45.50.-j, 51.10.+y

I. INTRODUCTION

There has been a lot of interest in the flow of a granular material down an inclined plane, because large scale simulations [1] have been able to provide a detailed description of the dynamics within the flow which was not previously accessible in experiments. The simulations reveal several surprising features. It is found that the volume fraction in the bulk of the flow is a constant, independent of total height and of conditions at the bottom boundary, and dependent only on the angle of inclination. There have been some simulation studies [2] which have also indicated that the constitutive relations derived from kinetic theory are valid for these flows, while other studies [3–5] suggest that long-range correlations are important and kinetic theory cannot be applied for these flows. All the components of the stress are found to be proportional to obey the Bagnold law, which states that the stress is the square of the strain rate,

$$\sigma_{ij} = B_{ij} \dot{\gamma}^2, \quad (1)$$

where the Bagnold coefficients, B_{ij} , which have dimensions of $(\text{mass})(\text{length})^{-1}$, are functions of the volume fraction. The Bagnold law is a dimensional necessity if the only time scale in the flow is the inverse of the strain rate, and the period of particle interactions does not influence the flow dynamics. Note that the gravitational acceleration does not provide a material time scale. It cannot enter into the constitutive relation for the stress, because the gravitational acceleration is a body force, whereas the stress is a surface force generated by the local strain rate. In other words, the constitutive relation must be independent of whether the material is deformed with gravity or without. In the present problem, the gravitational acceleration provides the applied force per unit volume, which is balanced by the divergence of the stress; the stress is provided by the constitutive relation which is not dependent on gravity. Since collisions are due to the fluctuating velocity of the particles, the collision frequency must be related to the fluctuating velocity, which in turn is related

to the strain rate through the energy balance equation (note that the conduction term is neglected in the energy balance equation when the length scale is large compared to the conduction length). If the period of particle interactions is small compared to the inverse of the strain rate, collisions can be considered instantaneous, and there is no material time scale. Therefore, the only time scale is the inverse of the strain rate, and the stress must be proportional to the square of the strain rate. The fact that simulations do observe that the stress is proportional to the square of the strain rate suggests that results from the kinetic theory calculations [6–11] may be applicable for dense granular flows down an inclined plane.

The applicability of constitutive relations from kinetic theory [6–11] for dense granular flows is a contentious issue, because some specific assumptions made in deriving constitutive relations from the Enskog equation do not seem to be applicable for dense flows. For example, we have the following:

(1) The collision integral in the Boltzmann and Enskog equations assume two-body interactions between particles. For dense granular flows, it is assumed that multibody contacts are the dominant mode of interaction.

(2) Correlations in the particle positions are incorporated in an approximate way using the pair distribution function, and the correlations in the velocities are neglected in kinetic theory.

The latter issue has been examined by Kumaran [13], where it is shown that the dispersion relations for the hydrodynamic modes in the shear flow of inelastic particles is very different from that in an elastic fluid. In particular, the long time tails in the velocity autocorrelation functions are not present in a granular fluid because energy is a nonconserved variable in a granular fluid. It is known that hydrodynamic correlations in an elastic fluid do alter the form of the constitutive relations derived by kinetic theory [12], resulting in a divergent viscosity in two dimensions and divergent Burnett coefficients in three dimensions. However, these divergences are not present for a system of inelastic particles [13], if the Green-Kubo relations are used to calculate the trans-

port coefficients. The applicability of Green-Kubo relations to a system far from equilibrium is not certain, and a more detailed calculation using the ring kinetic approximation is required to ascertain the effect of long time tails on the transport coefficients in these systems.

In the present analysis, we consider a three-dimensional dense granular flow of particles with volume fraction in the range 0.52 to 0.59. We first examine the issue of multibody contacts in a dense granular flow by evaluating the dependence of the coordination number on the stiffness of particles. The equivalent spring constant for materials such as sand or glass beads is of the order of 10^7 N/m or more, whereas most simulations are carried out with a spring constant of order 10^3 N/m for computational efficiency. Silbert *et al.* [14] studied the contact lifetime distributions of dense granular flows using the DEM method for relatively soft particles with spring constant of order 10^3 N/m, and found that the dominant mode of interaction is brief binary collisions, rather than a large number of long-lived contacts. This indicates that the binary collision approximation is, in fact, a good approximation for dense granular flows. In the present study, we examine whether the coordination number changes significantly when the stiffness of particle contacts is increased.

In the present analysis, we use a rough particle collision model, in which the post-collisional relative velocity normal to the surfaces at contact is $-e_n$ times the precollisional normal relative velocity, and the post-collisional relative velocity tangential to the surfaces at contact is $-e_t$ times the precollisional relative tangential velocity. The normal coefficient of restitution e_n varies between 0 and 1; $e_n=1$ corresponds to perfectly elastic collisions, while $e_n=0$ corresponds to perfectly inelastic collisions. The tangential coefficient of restitution e_t varies between -1 and $+1$, $e_t=-1$ corresponds to smooth particles where there is no change in the relative velocity after collision, while $e_t=1$ corresponds to perfectly rough particles where the relative velocity perpendicular to the line joining centers is reversed after the collision. Energy is conserved for both $e_t=+1$ and $e_t=-1$, and it is convenient to carry out an asymptotic analysis about the limit where energy is conserved. Detailed measurements of particle collisions (see, for example, Foerster [15]) indicate that there are two types of collisions depending on the angle between the relative velocity vector and the line joining centers. Head-on collisions are found to be sticking collisions, where the asperities on the particles lock during a collision. The impulse tangential to the colliding surfaces is proportional to the relative tangential velocity at the point of contact. Grazing collisions are found to be sliding collisions, where the tangential impulse is equal to the coefficient of friction times the normal impulse. While sticking collisions can be incorporated with relative ease in kinetic theory calculations, it is difficult to obtain analytical results for the constitutive relations for sliding collisions. It was possible to obtain results for a partially rough collision model in an earlier paper [11], where head-on collisions were considered rough, while grazing collisions were considered smooth. In the present, we consider all collisions to be rough and characterized by just one normal and one tangential coefficient of restitution, in order to facilitate a quantitative comparison between theory and simulations.

This analysis shows that the average coordination number is less than 1 with $[k_n/(mg/d)]=10^8$, even when the angle of inclination is only 1° greater than the angle of repose (for comparison, $[k_n/(mg/d)]\sim 10^{10}$ for $100\ \mu\text{m}$ particles of sand or glass). This indicates that the binary collision approximation is valid for granular flows of materials of practical interest. We then numerically compare the coefficients in the constitutive relations for the different components of the stress obtained from soft particle discrete element (DE) simulations, hard particle event driven (ED) simulations, and from kinetic theory [11]. It is found that the Bagnold coefficients obtained by theory, ED and DE simulations are in quantitative agreement, to within about 40% for the normal stress and about 20% for the shear stress, even when the Bagnold coefficient varies by more than an order of magnitude, provided the pair distribution function at contact obtained from simulations is used in the theory. It is also found that the pair distribution function obtained from simulations is much higher than the equilibrium pair distribution function of an elastic hard sphere system by an order of magnitude or more. Therefore, the Bagnold coefficients obtained using the equilibrium pair distribution function are likely to be significantly in error. Finally, we examine the reason why the Bagnold coefficients in the DE simulations do not change very much when the spring constant varies by about three orders of magnitude between $[k_n/(mg/d)]=10^5$ (for which particle interactions are by multibody contacts) and $[k_n/(mg/d)]=10^8$ (where particle interactions are primarily due to binary contacts). In the multibody contact regime, we determine the magnitudes of all the forces acting instantaneously on a particle, and calculate the ratio of the forces with the second largest and the largest magnitudes. In a static regime, it is expected that this ratio is $O(1)$, since a static equilibrium is due to all the forces acting on a particle. In a flowing state with $[k_n/(mg/d)]=10^5$, it is found that this ratio is smaller than 1, indicating that the net force on the particle is primarily due to one contact. This indicates that the binary contact approximation may be valid even when the coordination number is larger than 1.

II. CONSTITUTIVE RELATIONS

The basic equation used is the inelastic Enskog equation, and the details of the derivation have been discussed earlier [10,11]. The velocity distribution function is assumed to be an anisotropic Gaussian in both the linear and angular velocities. An expansion is carried out about the elastic limit in the parameter $\varepsilon=(1-e_n)^{1/2}$, where e_n is the coefficient of restitution. In the case of rough particles, the ratio $(1-e_t)/(1-e_n)$ is considered to be $O(1)$ in the expansion. The leading order, $O(\varepsilon)$ and $O(\varepsilon^2)$ equations are solved to obtain the corresponding distribution functions. The constitutive relations are then determined from the solutions for the distribution function. In the expansion, we retain all terms up to $O(\varepsilon^2)$ smaller than the leading order pressure, and neglecting terms $O(\varepsilon^3)$ and higher, where $\varepsilon=(1-e_n)^{1/2}$. The viscous stress is $O(\varepsilon)$ smaller than the pressure, while the correction to the viscosity is $O(\varepsilon^2)$ smaller than the viscosity. There-

fore, the correction to the viscous stress due to inelasticity is $O(\varepsilon^3)$ smaller than the pressure. The latter is neglected, and so the viscosity is identical to that for an elastic system. Similarly, the Burnett terms proportional to the square of the strain rate are $O(\varepsilon^2)$ smaller than the leading order pressure, and the corrections to the Burnett terms due to inelasticity are $O(\varepsilon^2)$ smaller than the Burnett terms, or $O(\varepsilon^4)$ smaller than the pressure. Therefore, these are also neglected. The viscometric coefficients obtained in this manner are approximate due to the assumption that the solution is an anisotropic Gaussian. This approximation is equivalent to retaining the leading term in the Sonine polynomial expansion for the first and second corrections to the distribution function. In the calculation of the viscous stress, for example, the correction to the distribution function due to mean shear is of the form [16] $f_{\text{MB}} G_{ij} [c_i c_j - (\delta_{ij} c^2/3)] B(|\mathbf{c}|)$, where \mathbf{c} is the fluctuating velocity, f_{MB} is the Maxwell-Boltzmann distribution, G_{ij} is the strain rate, and B is a function of the absolute value of the fluctuating velocity. A Sonine polynomial expansion is then used for the function $B(|\mathbf{c}|)$. In the Gaussian approximation [11], when an anisotropic Gaussian function of the fluctuating velocity is expanded about a Maxwell-Boltzmann distribution, it is equivalent to assuming that the function B is a constant, so that only the leading term in the expansion is retained. A similar approximation is used for the second correction to the distribution function, which provides the Burnett terms in the equation for the stress that are quadratic functions of the strain rate. We neglect terms proportional to the gradient of the strain rate for reasons explained below. For an elastic gas of smooth particles, a comparison of the results obtained using the Gaussian approximation [10] with that obtained using the Sonine polynomial expansion [16] indicated that the error in the viscosity due to the neglect of the next higher term is 1.2%, and the error in the Burnett coefficients is about 6%.

We use a uniform approximation for the constitutive relation which is valid in the limits where the length scale is large and small compared to the conduction length. We discuss the constitutive relations appropriate for both these limits first, and then the uniform approximation is provided. The mass of a particle is set equal to 1 in the present calculation, so that all parameters are nondimensionalized by particle mass, and the temperature has units of the square of velocity. The conduction length is determined by a balance between the rates of thermal diffusion and dissipation. The divergence of the heat flux is $\rho D_T (T/L^2)$, where T is the temperature, L is the length scale over which the temperature varies. The thermal diffusivity $D_T \sim \lambda T^{1/2}$, where λ is the microscopic scale (mean free path in a dilute gas and particle diameter in a dense gas). The rate of dissipation is proportional to $(\rho \varepsilon^2 T^{3/2}/\lambda)$, since dissipation of energy in a collision is proportional to $(1 - e_n)T$, and the collision frequency is proportional to $(T^{1/2}/\lambda)$. A balance between the rates of conduction and dissipation is obtained only for $L = \delta \sim (\lambda/\varepsilon)$, where δ is the conduction length.

If the macroscopic scale, which is the height of the flowing layer h in the present system, is large compared to the conduction length, the rate of conduction of energy is small compared to the rate of dissipation. The temperature is de-

termined by a local balance between the rates of production and dissipation, and the energy balance reduces to

$$2\mu S_{ij} S_{ji} - D = 0, \quad (2)$$

where μ is the viscosity, S_{ij} is the symmetric part of the rate of deformation tensor G_{ij} , and D is the rate of dissipation of energy. The stress is expressed in terms of the symmetric part S_{ij} , the antisymmetric part A_{ij} , and the isotropic part of the rate of deformation tensor G_{ij} , as well as in terms of the temperature gradients. The most general expression for the stress obtained using the leading order, first and second corrections to the distribution function is [16]

$$\begin{aligned} \sigma_{ij} = & -p(\phi, S_{ij}, G_{ii}) \delta_{ij} + 2\mu(\phi, S_{ij}, G_{ii}) S_{ij} + \mu_b(\phi, S_{ij}, G_{ii}) \delta_{ij} G_{kk} \\ & + \mathcal{A}_{SS} S_{ik} S_{kj} + \mathcal{A}_{SG} S_{ij} G_{kk} + \mathcal{A}_{SAS}(S_{ik} A_{kj} + S_{jk} A_{ki}) \\ & + \mathcal{A}_{AA} A_{ik} A_{kj} + \mathcal{A}_{SAA}(A_{ik} S_{kj} - S_{ik} A_{kj}) + \mathcal{C}_S \left[\frac{\partial}{\partial x_i} \left(\frac{1}{\rho} \frac{\partial p}{\partial x_j} \right) \right. \\ & + \frac{\partial}{\partial x_j} \left(\frac{1}{\rho} \frac{\partial p}{\partial x_i} \right) - \frac{2\delta_{ij}}{3} \frac{\partial}{\partial x_k} \left(\frac{1}{\rho} \frac{\partial p}{\partial x_k} \right) \left. \right] + \frac{\delta_{ij}}{3} \left[\mathcal{B}_{SS} S_{kl} S_{lk} \right. \\ & + \mathcal{B}_{AA} A_{kl} A_{lk} + \mathcal{B}_{GG} G_{kk}^2 + \mathcal{C}_I \frac{\partial}{\partial x_k} \left(\frac{1}{\rho} \frac{\partial \sigma_{kl}}{\partial x_l} \right) \left. \right] \\ & + \mathcal{C}_A \left[\frac{\partial}{\partial x_j} \left(\frac{1}{\rho} \frac{\partial p}{\partial x_i} \right) - \frac{\partial}{\partial x_i} \left(\frac{1}{\rho} \frac{\partial p}{\partial x_j} \right) \right] + \mathcal{D} \left(\frac{\partial}{\partial x_i} \frac{\partial}{\partial x_j} \right. \\ & - \frac{\delta_{ij}}{3} \frac{\partial^2}{\partial x_k^2} \left. \right) T + \frac{\mathcal{E}}{T} \left(\frac{\partial T}{\partial x_i} \frac{\partial T}{\partial x_j} - \frac{\delta_{ij}}{3} \frac{\partial T}{\partial x_k} \frac{\partial T}{\partial x_k} \right) + \frac{\mathcal{F}}{\rho T} \left(\frac{1}{2} \frac{\partial p}{\partial x_i} \frac{\partial T}{\partial x_j} \right. \\ & \left. + \frac{1}{2} \frac{\partial T}{\partial x_i} \frac{\partial p}{\partial x_j} - \frac{\delta_{ij}}{3} \frac{\partial T}{\partial x_k} \frac{\partial p}{\partial x_k} \right). \quad (3) \end{aligned}$$

Note that the mass of the particle has been set equal to 1 without loss of generality, and from dimensional analysis, all the Burnett coefficients above have dimensions of inverse length. In the above equation, we retain the pressure and the viscous terms, and the Burnett terms proportional to \mathcal{A} and \mathcal{B} , and neglect all other terms, for the following reason. The Burnett terms proportional to \mathcal{A} and \mathcal{B} are proportional to the square of the strain rate, $\dot{\gamma}^2$. The terms proportional to \mathcal{C} to \mathcal{F} are all proportional to (T/h^2) , where h is the macroscopic scale. The temperature and strain rate can be compared by examining the energy balance equation (2), in which the viscosity is proportional to $(T^{1/2}/d^2)$, and the rate of dissipation of energy per unit volume is proportional to $(\rho \varepsilon^2 T^{3/2}/\lambda)$. For a dense flow, $\rho \sim (1/d^3)$, and $\lambda \sim d$, so the temperature scales as $T \sim (\dot{\gamma} d/\varepsilon)^2 \sim (\delta \dot{\gamma})^2$. This can be used to compare the terms proportional to the square of the strain rate and the temperature gradient in Eq. (3). The terms proportional to the strain rate scale as $\dot{\gamma}^2$, while those proportional to the second spatial derivative of the temperature and pressure scale as $(\dot{\gamma} \delta/h)^2$, where h , the height of the flowing layer, is the macroscopic length scale in the present problem. For $(\delta/h) \ll 1$, the terms proportional to the second derivative of the temperature can be neglected compared to the terms proportional to the square of the strain rate. Therefore, we retain the terms proportional to \mathcal{A} and \mathcal{B} in Eq. (3), and neglect all other terms. The expression used for the stress is

$$\begin{aligned} \sigma_{ij} = & -p\delta_{ij} + 2\mu S_{ij} + \mu_b \delta_{ij} G_{kk} + \mathcal{A}_{SS} S_{ik} S_{kj} + \mathcal{A}_{SG} S_{ij} G_{kk} \\ & + \mathcal{A}_{SAS}(S_{ik} A_{kj} + S_{jk} A_{ki}) + \mathcal{A}_{AA} A_{ik} A_{kj} + \mathcal{A}_{SAA}(A_{ik} S_{kj} \\ & - S_{ik} A_{kj}) + \frac{\delta_{ij}}{3} (\mathcal{B}_{SS} S_{kl} S_{lk} + \mathcal{B}_{AA} A_{kl} A_{lk} + \mathcal{B}_{GG} G_{kk}^2). \end{aligned} \quad (4)$$

The reason the terms proportional to \mathcal{A} and \mathcal{B} are retained here are twofold. First, it has been shown [10] that the decay rates of the hydrodynamic modes in a uniformly sheared granular flow depend on the coefficients \mathcal{A} and \mathcal{B} in the long wave limit. In the present system, the terms proportional to \mathcal{A} and \mathcal{B} are necessary to capture the normal stress differences. It has been observed in simulations [1] that the first normal stress difference is close to zero in these flows, but the second normal stress difference is significant. We examine whether the predictions are in agreement with the observations by retaining the normal stress terms: The pressure, viscosity and the coefficients \mathcal{A} and \mathcal{B} from an earlier calculation [11]. Not all of these coefficients are required for the present calculation, since we are considering a unidirectional flow in which the isotropic part of the rate of deformation tensor is zero. The equations for the components of the stress tensor are

$$\begin{aligned} \sigma_{xy} &= \mu \dot{\gamma}, \\ \sigma_{xx} &= -p + b_{xx} \dot{\gamma}^2, \\ s_{yy} &= -p + b_{yy} \dot{\gamma}^2, \\ s_{zz} &= -p + b_{zz} \dot{\gamma}^2. \end{aligned} \quad (5)$$

The theory predicts that the coefficients b_{xx} and b_{yy} differ by less than 1%, so separate expressions are not provided for these coefficients. However, there is a significant difference between b_{xx} and b_{zz} . Note that the coefficients b_{ij} in Eq. (5) are not the same as B_{ij} in Eq. (1). In Eq. (5), the pressure is proportional to the temperature, which in turn is proportional to the strain rate due to Eq. (2). Therefore, for the normal stress terms, the ratio of the pressure and the square of the strain rate is included in the coefficient B_{ij} in Eq. (1). In a similar manner, for the shear stress, the viscosity is proportional to the square root of the temperature, which in turn is proportional to the strain rate due to the energy Eq. (2). Therefore, the ratio of the viscosity and strain rate is included in the definition of B_{xy} in Eq. (1).

It is convenient to express the viscometric coefficients and the dissipation coefficients as a product of two functions, one of which is a dimensionless function of volume fraction, and the other is a product of suitably chosen powers of the granular temperature and particle diameter, the latter having the same dimensions as the viscometric function under consideration. (Note that the granular temperature has dimensions of the square of the velocity, since the mass is set equal to 1.) From dimensional analysis, it can be inferred that pressure p is proportional to (T/d^3) , the viscosity μ and thermal conductivity K are proportional to $(T^{1/2}/d^2)$, and rate of dissipation of energy D is proportional to $(\rho^2 T^{3/2})$, where ρ is the number density, and therefore we write

TABLE I. Viscometric coefficients obtained from kinetic theory for rough nearly elastic spheres in three dimensions [11]. Here, $a_t = (1 - e_t)/(1 - e_n)$. It should be noted that in the above relations, particle mass is set equal to 1.

	Rough
p_ϕ	$(6\phi/\pi)[1 + 2(2 - \varepsilon^2)\phi\chi]$
μ_ϕ	$(0.195/\chi) + 0.892\phi + 3.112\phi^2\chi$
D_ϕ	$(144/\pi^{3/2})\phi^2\chi(1 + a_t)$
K_ϕ	$(1.014/\chi) + 5.015\phi + 19.27\phi^2\chi$
$b_{\phi xx}$	$(0.04094/\chi) + (0.00433/\phi\chi^2)$ $- 0.191\phi - 1.05\phi^2\chi$
$b_{\phi zz}$	$(0.0300698/\chi) + (0.00132835/\phi\chi^2)$ $+ 0.0212626\phi - 0.280498\phi^2\chi$

$$p = p_\phi(T/d^3),$$

$$\mu = \mu_\phi(\phi)(T^{1/2}/d^2),$$

$$b_{xx} = b_{\phi xx}(\phi)(1/d),$$

$$b_{yy} = b_{\phi yy}(\phi)(1/d),$$

$$b_{zz} = b_{\phi zz}(\phi)(1/d),$$

$$K = K_\phi(\phi)(T^{1/2}/d^2),$$

$$D = D_\phi(\phi)\varepsilon^2(T^{3/2}/d^6), \quad (6)$$

where the temperature is obtained in terms of the strain rate using the energy balance equation. The values of these coefficients obtained in an earlier calculation [11] which are used here are shown in Table I. As already mentioned, the difference between $b_{\phi xx}$ and $b_{\phi yy}$ is very small, and so we assume $b_{\phi xx} = b_{\phi yy}$ in the present calculation.

The theoretical expressions for the pressure, viscosity, and Burnett coefficients are provided in Table I. Using the energy balance Eq. (2), the relation between temperature and strain rate is determined. This is inserted into Eq. (6) to determine pressure and viscosity in terms of strain rate. These are then inserted into Eq. (5), and the resulting stress is divided by the square of the strain rate, to determine the Bagnold coefficients.

III. SIMULATION TECHNIQUES

Two types of simulation techniques are used. The first is the discrete element (DE) simulations of the flow down an inclined plane of spherical particles, in which the contact force between overlapping particles is modeled by a combination of a linear spring and a dashpot. The configuration and coordinate system for the flow down an inclined plane are shown in Fig. 1. Here, x and y are the flow and gradient directions, while the z direction is perpendicular to the plane of the flow. The height of the flowing layer was set equal to 40 particle diameters for all the results reported here, and the

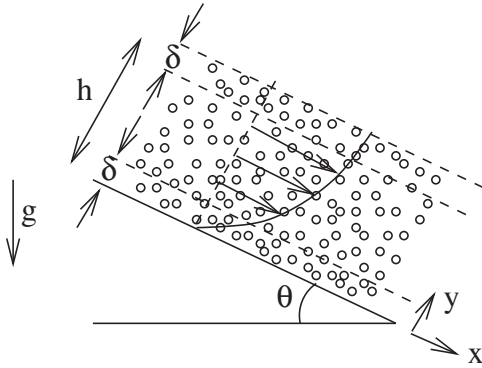


FIG. 1. Configuration and coordinate system for the DEM simulations for the flow down an inclined plane.

simulation cell contains 20 particles in the flow directions, 10 particles in the spanwise direction, and periodic boundary conditions are used in the flow and spanwise directions. While calculating the Bagnold coefficients, we restrict attention to the central region of the flow of the width of 20 particle diameters, and do not include regions at the top and bottom of the thickness of 10 particle diameters. This is because, as explained earlier, the temperature and stress fields in boundary layers of thickness comparable to the conduction length at the top and bottom boundaries are influenced by the energy boundary conditions at these boundaries. The rate of conduction of energy is of the same magnitude as the rates of production and dissipation in the boundary layers, and the Bagnold law is not valid. Therefore, we exclude these boundary layers while calculating the Bagnold coefficients.

The force model used is the linear contact force model of Silbert *et al.* [1] without friction, since this results in velocity independent coefficients of restitution. This facilitates quantitative comparisons with earlier results [11] which were derived assuming velocity independent coefficients of restitution. However, we consider only the linear contact model, and we do not include static friction in the model. This is because we would like to make a numerical comparison between the results of DE simulations and kinetic theory for the same contact model, and frictional contacts are difficult to incorporate in kinetic theory calculations, while a nonlinear contact model results in velocity dependent coefficients of restitution. The contact model contains spring and damping constants, (k_n, k_t) and (γ_n, γ_t) , in the tangential and normal directions. Of these, one spring and damping constant, k_n and γ_n , are for displacements normal to the surface of contact, while the other spring and damping constant, k_t and γ_t , is for displacements tangential to the surface of contact. In the simulations, we set $k_t = (2/7)k_n$, and adjust γ_n and γ_t so that both the tangential and normal coefficients of restitution are 0.9. The relation between the coefficients of restitution and the spring and damping constants are given in Silbert *et al.* [1].

In addition to the DE simulations, we also use the ED simulations of the simple shear flow in the absence of gravity in order to obtain the Bagnold coefficients. In this simulation technique, the interaction between particles are modeled as instantaneous contacts, in which the post-collisional relative

velocity normal to the surface of contact is $-e_n$ times the precollisional relative normal velocity, and the post-collisional relative velocity tangential to the surface of contact is $-e_t$ times the precollisional relative tangential velocity. Here, e_n is the normal coefficient of restitution and e_t is the tangential coefficient of restitution. Both e_n and e_t are set equal to 0.9 in the present simulations, so that the DE and ED models are identical to each other for binary collisions.

The results reported here were carried out in a cubic box using 500 particles. All simulations were averaged over 2×10^4 collisions per particle, after an initial equilibration run which extended over a time period corresponding to 2×10^4 collisions per particle. For very small system sizes, when the system is sheared, it attains in-plane ordering for the volume fractions considered here, and the structure is not random. As the system size is increased, the ordered state becomes unstable and undergoes a transition to a random state. It is this random state that is of interest in the present analysis, so we have taken care to ensure that the structure is actually random in both ED and DE simulations. Therefore, we have taken care to ensure that the flowing solid is disordered, that is, there is no icosahedral order or in-plane order as inferred from the respective order parameters. In two dimensions, the hexagonal order parameter for particles in contact is defined by [18]

$$q_m = \langle \exp(im\theta_p) \rangle, \quad (7)$$

where $\langle \dots \rangle$ is the average over all the bonds in the system and θ_p is the angle, in the x - z plane, formed by a bond with respect to some arbitrary axis. For a hexagonal close packed system, q_6 is unity, and is lower otherwise. For the present hard sphere system, we define the order parameter q_m as the sum over all binary collisions, since the particles are in contact only at collision. Thus, the order parameter q_m is defined as [18]

$$q_m = \frac{1}{N_{\text{col collisions}}} \sum \exp(im\theta), \quad (8)$$

where N_{col} is the number of collisions, and the above average is carried out over all collisions.

In three dimensions, the presence of icosahedral ordering can be inferred from the three-dimensional order parameter Q_l , which is defined as

$$Q_l = \left(\frac{2l+1}{4\pi} \sum_{m=-l}^l |\langle Y_{lm}(\theta, \phi) \rangle|^2 \right)^{1/2}, \quad (9)$$

where $Y_{lm}(\theta, \phi)$ is the spherical harmonic,

$$Y_{lm}(\theta, \phi) = \sqrt{\frac{2l+1}{4\pi}} P_l^m[\cos(\theta)] \exp(im\phi), \quad (10)$$

θ and ϕ are the azimuthal and meridional angles in a spherical coordinate system with an arbitrary axis, and P_l^m are the Legendre polynomials. For systems with perfect icosahedral ordering, Q_6 is greater than 0.5, whereas it is zero for random structures. Therefore, Q_6 can be used to distinguish between random and ordered crystalline structures.

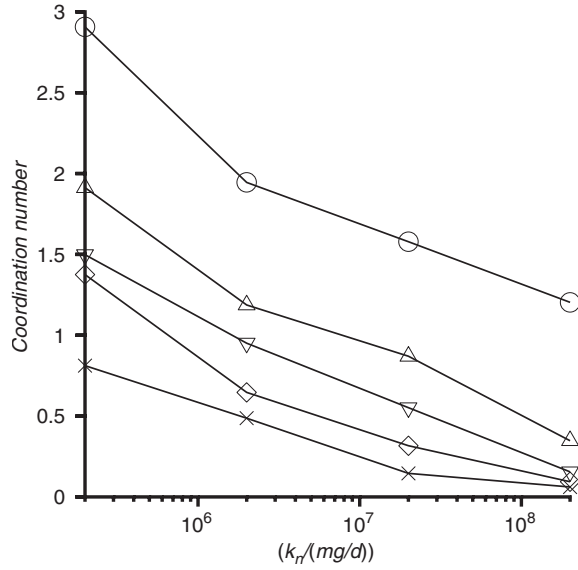


FIG. 2. The average coordination number as a function of the spring constant at different angles of inclination obtained using DEM simulations. ○, 21°; △, 22°; ▽, 23°; ◇, 24°; ×, 25°.

In the present simulations with 500 particles, Q_6 is 0.03 at the highest volume fraction of 0.57, while q_6 is less than 0.01. This indicates that there is no ordering in the relative arrangement of particles. We have also done a size check by analyzing a 2048 particle system as well, and the results do not change by more than 2%. One of the difficulties in event driven simulations at large volume fractions is the advent of inelastic collapse [19], where there is an infinite number of collisions in a finite time period. This results in overlap between particles due to numerical errors. In the present simulations, we find that there are one or two particle overlaps when the volume fraction in three dimensions is 0.58, and the number of overlaps increases as the volume fraction is increased beyond 0.58. Therefore, we have restricted the comparisons with event driven simulations with volume fraction 0.57 and lower. The difficulty with inelastic collapse is not present in DE simulations, and so we are able to extend the DE simulations to volume fraction up to 0.59 for the flow down an inclined plane.

IV. RESULTS

First, we examine the average coordination number in the dense granular flow down an inclined plane. For the microscopic model used here, the angle of repose is 20°, flow starts when the angle of inclination is 21°, and the flow becomes unstable when the angle of inclination increases beyond 25°. Figure 2 shows the average coordination number as a function of the scaled spring constant $[k_n/(mg/d)]$, where m and d are the mass and diameter of the particle, and g is the acceleration due to gravity. It is observed that the average coordination number is large for soft materials with $[k_n/(mg/d)]=2 \times 10^5$, but it decreases below 1 for harder materials with $[k_n/(mg/d)]=2 \times 10^8$ for all angles of inclination above 21°. Even at 21°, the coordination number de-

creases below 1.5 at $[k_n/(mg/d)]=2 \times 10^8$, and the trends indicate that it will increase below 1 for $[k_n/(mg/d)]=10^{10}$ or more. Thus, it is clear that the binary collision mechanism is the dominant particle interaction mechanism in relatively hard particle systems of practical interest.

It is rather surprising that binary collisions dominate in a dense flow. However, it is important to understand that the particles in a granular flow are very stiff, in contrast to the soft Lennard-Jones-type potentials used for molecular fluids. In the limit of perfectly hard particles (infinite spring constant), the pair potential is infinite when the distance between particles is smaller than the sum of their radii, and zero otherwise. Consequently, in this limit, all interactions are instantaneous, and all particle interactions are binary interactions, even in a dense flow. For a linear contact model in which the spring constant is high but not infinite, the time period of a collision is $\tau_c = \pi[(2k_n/m) - (\dot{\gamma}^2/4)]^{-1/2}$, and this time period decreases as the spring constant increases. Note that the time period of a collision is a material time scale, which depends only on the properties of the materials used in the simulations. The flow time scale is the time between collisions, or the inverse of the collision frequency ν_c . In a dense granular flow, the collision frequency scales as $(\chi\dot{\gamma}^{-1})$, where χ is the pair distribution function at contact and $\dot{\gamma}$ is the strain rate. One would expect a transition from a multibody contact regime to a binary collision regime as k_n is increased for $\tau_c\nu_c \sim 1$. To make a numerical comparison, we evaluate the collision frequency ν_c using the ED simulation for the same volume fraction as that in the flow down an inclined plane. Using the expression for the period of a collision, we then evaluate the value of $[k_n/(mg/d)]$ at which $\nu_c\tau_c=1$. The results of the calculation show that for 25°, $\tau_c\nu_c=1$ at $[k_n/(mg/d)]=1.5 \times 10^4$, while at 21°, $\tau_c\nu_c=1$ at $[k_n/(mg/d)]=2 \times 10^6$. As noted earlier, the value of $[k_n/(mg/d)]=10^{10}$ or more for materials such as glass spheres and steel balls with diameters 100 μ –1 mm, and therefore we would expect binary collisions to dominate even for 21° at the initiation of flow for these materials.

Next, we compare the numerical values of the Bagnold coefficients obtained from theory with those from ED and DE simulations using Eq. (1). As mentioned earlier, the DE simulations are carried out for the flow down an inclined plane, and the stresses are measured in the bulk of the flow where the volume fraction is a constant. The ED simulations are carried out for a simple shear flow in the absence of gravity. In the theory, we use the pair distribution function evaluated from the ED simulations. The pair correlation function at contact, g_c , is determined in two ways. The first is to calculate the actual radial distribution function as a function of radius, and find the radial distribution function at contact by extrapolation. For this, the region between $r=d$ and $r=3d$ in the radial direction around a particle was divided into 60 bins, and the probability of finding the particle in each bin was calculated. The radial distribution function obtained at $r=d$ was obtained by spline fitting. The second procedure is to use the relationship between g_c and the collision frequency ν using the expression [16]

$$\nu = 2\rho^2 g_c \sqrt{\pi T}, \quad (11)$$

where T , the granular temperature, is the mean square of the particle velocities, and ρ is the number density. Equation (11)

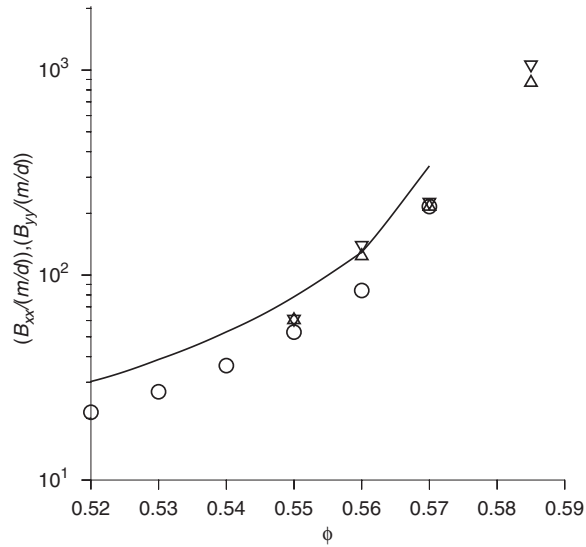


FIG. 3. The scaled Bagnold coefficients $[B_{xx}/(m/d)]$, $[B_{yy}/(m/d)]$ as a function of volume fraction. \circ , ED simulations; \triangle , DE simulations with $[k_n/(mg/d)]=2 \times 10^5$; ∇ , DE simulations with $[k_n/(mg/d)]=2 \times 10^8$; solid line, theory. The error bar in the estimation of the volume fraction in the DE simulations has an average value of 0.0043, and a maximum of 0.005.

is obtained from the kinetic theory for a gas of elastic spherical particles. It is known [17] that there is a correction to the above expression for inelastic particles. However, we find that this correction is less than 1% for the parameter values $e_t=e_n=0.9$ used here, and so we use [11] for calculating the pair distribution function in the present analysis.

This pair distribution function at contact is inserted into the theoretical expressions [11] in order to determine the theoretical values of the Bagnold coefficients. The Bagnold coefficients, scaled by (m/d) , are shown, along with the DE and ED results, in Figs. 3–5, where m and d are the particle mass and diameter. Here, x is the direction of flow along the inclined plane, y is the gradient direction perpendicular to the inclined plane, and z is the spanwise vorticity direction. The volume fraction cannot be fixed exactly in the DE simulations, since this is not a constant volume simulation. Therefore, the average volume fraction in the bulk of the flow, excluding a region of 10 particle diameters at the top and bottom, were used for the comparison. The standard deviation in the volume fraction in the DE simulations has a maximum value of 0.005 and an average value of 0.0043. The theoretical predictions as well as the DE and ED simulations show that the coefficients B_{xx} and B_{yy} differ by less than 1% over the range of volume fractions studied here, and the difference between these is smaller than the symbol size in Fig. 3, and so we do not show these separately. However, the Bagnold coefficient B_{zz} is lower than B_{xx} , as shown in Fig. 4, and the theory and simulations are in numerical agreement in this case as well. Figure 5 shows the component B_{xy} for the shear stress. Results could not be obtained from the ED simulations for volume fractions above 0.58, due to the advent of particle overlaps, and the maximum volume fraction in DE simulations was about 0.59. Figures 3–5 show that there is quantitative agreement between the theory, ED simu-

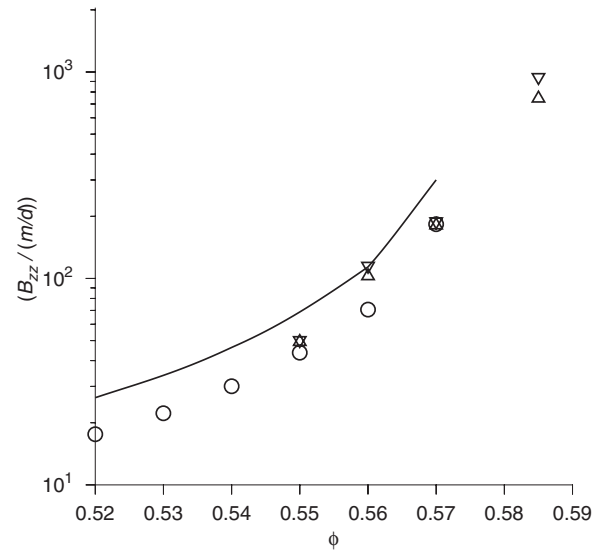


FIG. 4. The scaled Bagnold coefficient $[B_{zz}/(m/d)]$ as a function of volume fraction. \circ , ED simulations; \triangle , DE simulations with $[k_n/(mg/d)]=2 \times 10^5$; ∇ , DE simulations with $[k_n/(mg/d)]=2 \times 10^8$; solid line, theory. The error bar in the estimation of the volume fraction in the DE simulations has an average value of 0.0043, and a maximum of 0.005.

lations, and DE simulations, even though the Bagnold coefficients increase by more than an order of magnitude over the range of volume fractions considered. The difference between theory and ED simulations is only about 40% for the normal stresses, and about 20% for the shear stresses even though the Bagnold coefficients themselves increase by more than an order of magnitude. The DE simulations, which incorporate multibody collisions, are found to be in good

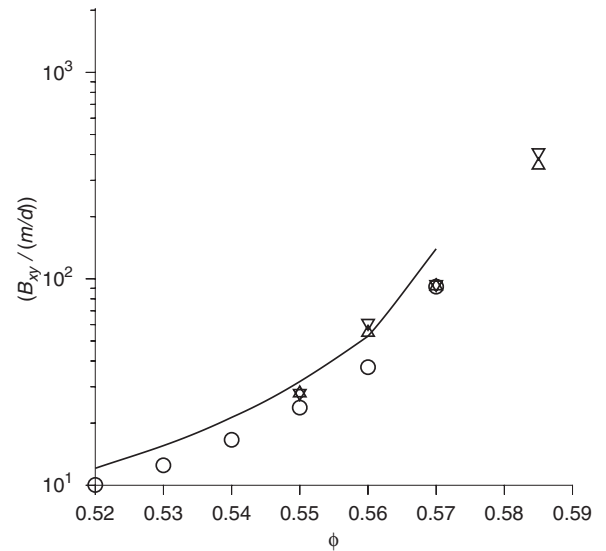


FIG. 5. The scaled Bagnold coefficient $[B_{xy}/(m/d)]$ as a function of volume fraction. \circ , ED simulations; \triangle , DE simulations with $[k_n/(mg/d)]=2 \times 10^5$; ∇ , DE simulations with $[k_n/(mg/d)]=2 \times 10^8$; solid line, theory. The error bar in the estimation of the volume fraction in the DE simulations has an average value of 0.0043, and a maximum of 0.005.

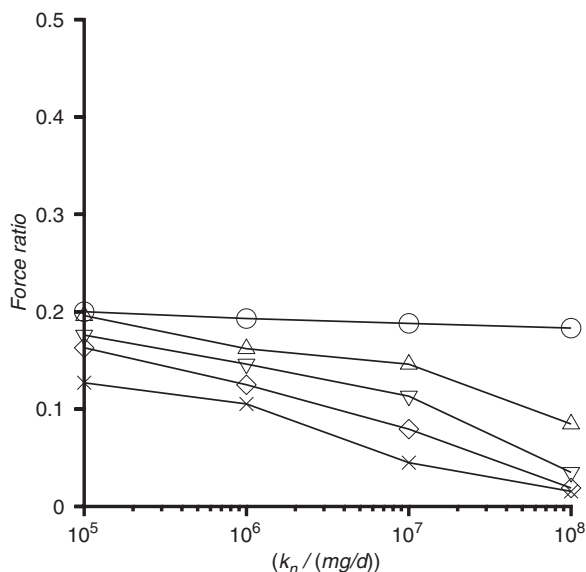


FIG. 6. The force ratio, which is defined as the average of the ratios of the magnitudes of the second largest and the largest forces acting on a particle, as a function of the angle of inclination for the flow down an inclined plane with $[k_n/(mg/d)]=2 \times 10^5$, $e_n=e_t=0.9$. \circ , $\theta=21^\circ$; \triangle , $\theta=22^\circ$; ∇ , $\theta=23^\circ$; \diamond , $\theta=24^\circ$; \times , $\theta=25^\circ$.

agreement with ED simulations, which have only binary collisions, in the dense region.

One surprising feature of the above results is that there is a variation of less than 20% between the Bagnold coefficients when $[k_n/(mg/d)]$ varies by three orders of magnitude. This is particularly surprising because there is a transition from a multiple contact regime to a binary collision regime, as indicated by the decrease in the coordination number in Fig. 2. One possible reason for this is that though there are multiple overlaps in the case of soft particles, there is one contact which exerts the largest force on the particle, and the force due to this contact is much larger than that due to all other contacts. In order to examine this, we measured the force ratio between the largest and the second largest force on the particles as follows. The magnitude of all the forces on the particles were determined, and the ratio of the magnitudes of the second largest force to the largest force was calculated. This was averaged over all the particles and over time. In particles with just one contact, the force ratio is zero, whereas one would expect the force ratio to be $O(1)$ in a quasistatic regime where all of the forces are nearly balanced with each other. The results for the force ratio for the flow down an inclined plane with $[k_n/(mg/d)]=[k_t/(mg/d)]=2 \times 10^5$ are shown in Fig. 6. The damping coefficients have been adjusted so that $e_t=e_n=0.9$. It is observed that the force ratio is about 0.2 even at 21° for this flow which has an angle of repose equal to 20° . This indicates that though there are multiple contacts for a particle, there is only one dominant contact at any instant of time. Though this does not explain why there is a very small variation in the Bagnold coefficients, it provides an indication why the binary collision approximation may be a good one even when there are multiple contacts.

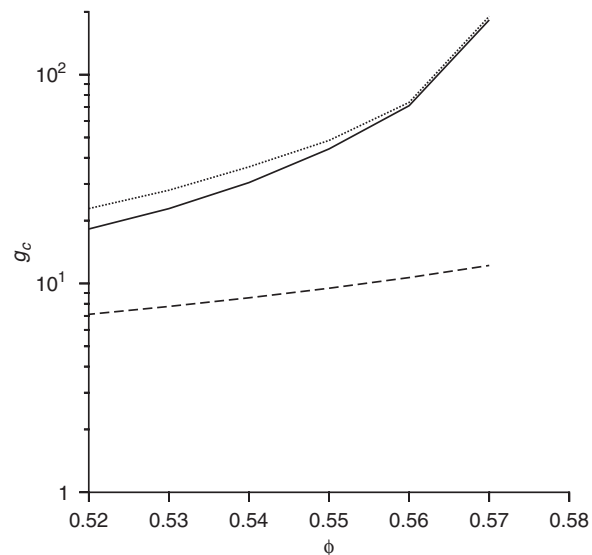


FIG. 7. The pair correlation function at contact, g_c , as a function of the volume fraction. The solid line shows the results from the ED simulation of a shear flow with $e_t=e_n=0.9$ obtained from the collision frequency using Eq. (11), the dotted line shows the result obtained by an extrapolation of the radial distribution function, and the broken line shows the correlation for equilibrium hard sphere fluids [21].

It should be noted that though there is good agreement between the theory and the DE and ED simulations, this is primarily because the theoretical calculation has incorporated the pair distribution function at contact determined from the simulations. It has been known [20] that the pair correlation function in a sheared system is different from that in an equilibrium system. Figure 7 shows a comparison between the pair distribution function from ED simulations for a sheared system with $e_t=e_n=0.9$, and the correlation by Torquato [21] for the pair distribution function in an equilibrium system,

$$g_c(\phi) = \frac{2 - \phi_f}{2(1 - \phi_f)^2} \frac{\phi_c - \phi_f}{\phi_c - \phi}, \quad (12)$$

where $\phi_c=0.64$ is the volume fraction at random close packing, and $\phi_f=0.49$ is the freezing volume fraction in three dimensions. The result obtained from the collision frequency using Eq. (11) is close to that obtained by extrapolation of the radial distribution function to $r=d$. However, it is observed that the pair correlation function for the sheared system is between one and two orders of magnitude larger than the pair correlation function for an equilibrium system. Thus, the use of the equilibrium pair correlation function in kinetic theory could result in poor comparison between theory and simulations, due to the error in the pair correlation function (Fig. 7).

The present analysis indicates that the binary collision approximation is a good one for dense granular flows. There is good quantitative agreement between the predictions of kinetic theory and numerical simulations, provided the pair correlation function from simulations are used in the theory,

and provided the collisions are nearly elastic. This is expected, since the theory uses an expansion about the limit of elastic collisions. There has been some recent work by Mitarai and Nakanishi [22] which suggests that the constitutive relations may need to be modified when the collisions be-

come highly inelastic. We are currently examining how the theory can be modified for highly inelastic collisions.

This research was supported by Swarnajayanthi, Department of Science and Technology, Government of India.

-
- [1] L. E. Silbert, D. Ertas, G. S. Grest, T. C. Halsey, D. Levine, and S. J. Plimpton, *Phys. Rev. E* **64**, 051302 (2001).
 - [2] N. Mitarai and H. Nakanishi, *Phys. Rev. Lett.* **94**, 128001 (2005).
 - [3] D. Ertas and T. C. Halsey, *Europhys. Lett.* **60**, 931 (2002).
 - [4] G. Lois, A. Lemaitre, and J. M. Carlson, *Phys. Rev. E* **72**, 051303 (2005).
 - [5] J. T. Jenkins, *Phys. Fluids* **18**, 103307 (2006).
 - [6] S. B. Savage and D. J. Jeffrey, *J. Fluid Mech.* **110**, 255 (1981).
 - [7] J. T. Jenkins and M. W. Richman, *Arch. Ration. Mech. Anal.* **87**, 355 (1985).
 - [8] C. K. K. Lun, S. B. Savage, D. J. Jeffrey, and N. Chepurnyi, *J. Fluid Mech.* **140**, 223 (1984).
 - [9] N. Sela and I. Goldhirsch, *J. Fluid Mech.* **361**, 41 (1998).
 - [10] V. Kumaran, *J. Fluid Mech.* **506**, 1 (2004).
 - [11] V. Kumaran, *J. Fluid Mech.* **561**, 1 (2006).
 - [12] M. H. Ernst, B. Cichocki, J. R. Dorfman, J. Sharma, and H. van Beijeren, *J. Stat. Phys.* **18**, 237 (1978).
 - [13] V. Kumaran, *Phys. Rev. Lett.* **96**, 258002 (2006).
 - [14] L. E. Silbert, G. S. Grest, R. Brewster, and A. J. Levine, *Phys. Rev. Lett.* **99**, 068002 (2007).
 - [15] S. F. Foerster, M. Y. Louge, H. Chang, and K. Allia, *Phys. Fluids* **6**, 1108 (1994).
 - [16] S. Chapman and T. G. Cowling, *The Mathematical Theory of Non-Uniform Gases* (Cambridge University Press, Cambridge, 1970).
 - [17] V. Garzo and J. W. Dufty, *Phys. Rev. E* **59**, 5895 (1999).
 - [18] V. Senthil Kumar and V. Kumaran, *J. Chem. Phys.* **124**, 204508 (2006).
 - [19] S. McNamara and W. R. Young, *Phys. Rev. E* **50**, R28 (1994).
 - [20] W. Schafer, R. Lovenich, N. A. Fromer, and D. S. Chemla, *Phys. Rev. Lett.* **86**, 344 (2001).
 - [21] S. Torquato, *Phys. Rev. E* **51**, 3170 (1995).
 - [22] N. Mitarai and H. Nakanishi, *Phys. Rev. E* **75**, 031305 (2007).